Journal of Power Sources 196 (2011) 2187–2194

Contents lists available at ScienceDirect

Journal of Power Sources

journal homepage: www.elsevier.com/locate/jpowsour

# Use of natural binders and ionic liquid electrolytes for greener and safer lithium-ion batteries

G.T. Kim, S.S. Jeong, M. Joost, E. Rocca, M. Winter, S. Passerini*, A. Balducci**

*Institute of Physical Chemistry, University of Muenster, Corrensstr. 28/30, 48149 Muenster, Germany*

ARTICLE INFO

*Article history:*
Received 19 July 2010
Received in revised form
13 September 2010
Accepted 16 September 2010
Available online 1 October 2010

*Keywords:*
Lithium batteries
CMC
$LiFePO_4$
$Li_4Ti_5O_{12}$
Ionic liquid
$PYR_{14}FSI$

ABSTRACT

This manuscript reports on the development of a safe and green lithium-ion battery containing sodium salt of CarboxyMethylCellulose (CMC) as binder, lithium titanate ($Li_4Ti_5O_{12}$) as anodic active material, lithium iron phosphate ($LiFePO_4$) as cathodic active material and an electrolytic solution based on the ionic liquid N-butyl-N-methylpyrrolidinium bis(fluorosulfonyl)imide ($PYR_{14}FSI$). The battery showed, at room temperature, a very stable specific capacity of 140 mAh $g^{-1}$ constant for more than 150 cycles. This indicated that the introduction of low cost and environmentally benign binders, like CMC, and non-flammable electrolytes, such as $PYR_{14}FSI$, represents a viable strategy for the development of new, greener and safer lithium-ion batteries.



## 1. Introduction

Lithium ion batteries dominate the consumer portable electronic and telecommunications market and they are also indicated as the most promising option for the next generation of hybrid and electric vehicles (HV, EV). The wide deployment of lithium ion batteries in the automotive industry would have tremendous consequences on the battery-market and it would further strengthen the central role of these systems in the field of the energy storage. For that, considerable efforts are now focused on the development and realization of lithium ion batteries able to fulfil the requirement necessary for the application in HV and EV.

When the present lithium ion technology is considered, the safety of batteries appears to be one of the main drawbacks holding the introduction of this technology in HV and EV. The commercial systems nowadays available use electrolytes commonly based on organic carbonates (e.g. propylene carbonate, PC, ethylene carbonate, EC) but since these electrolytes are flammable their use poses a serious safety risk and strongly reduces the battery operative temperature range [1,2]. For these reasons, the replacement of non-flammable, non-volatile ionic liquids (ILs) (see Fig. 1) for the organic carbonates appears very promising.

ILs are generally comprise a bulky, asymmetrical organic cation and a weakly coordinating inorganic/organic anion. They represent today a very interesting new class of room temperature ionic fluids. The main advantages of ILs toward organic solvents are, in addition to the previously mentioned non-flammability and negligible vapor pressure, the high chemical and thermal stability and, in some cases, hydrophobicity. For that, ILs have attracted a large attention for use as "green" solvents and recently have been intensively investigated as electrolytes (or electrolyte components) for various electrochemical devices. In the last few years a large number of ILs have been proposed and tested in combination with several anodic and cathodic materials for lithium and lithium-ion batteries [3–12]. The results of these studies have shown that ILs can be successfully used as electrolytes in lithium ion batteries at the place of the conventional organic carbonates. Between the ILs recently proposed and investigated, the N-butyl-N-methylpyrrolidinium bis(fluorosulfonyl)imide ($PYR_{14}FSI$) appears as one of the most interesting. $PYR_{14}FSI$ displays high conductivity (>4 mS $cm^{-1}$ at 20 °C) and an electrochemical stability window wider than 5.5 V [13]. In addition, because of the presence of the anion $FSI^-$ it also displays SEI film forming abilities [14]. For these reasons, we considered this ionic liquid as the most attractive candidate for lithium ion battery electrolytes.

Another important aspect concerning safety and environmental impact of the present battery technology is related with the

* Corresponding author. Tel.: +49 251 8336026; fax: +49 251 8336032.
** Corresponding author. Tel.: +49 251 8336083; fax: +49 251 8336084.
*E-mail addresses:* stefano.passerini@uni-muenster.de (S. Passerini), andrea.balducci@uni-muenster.de (A. Balducci).

0378-7753/$ – see front matter © 2010 Elsevier B.V. All rights reserved.
doi:10.1016/j.jpowsour.2010.09.080

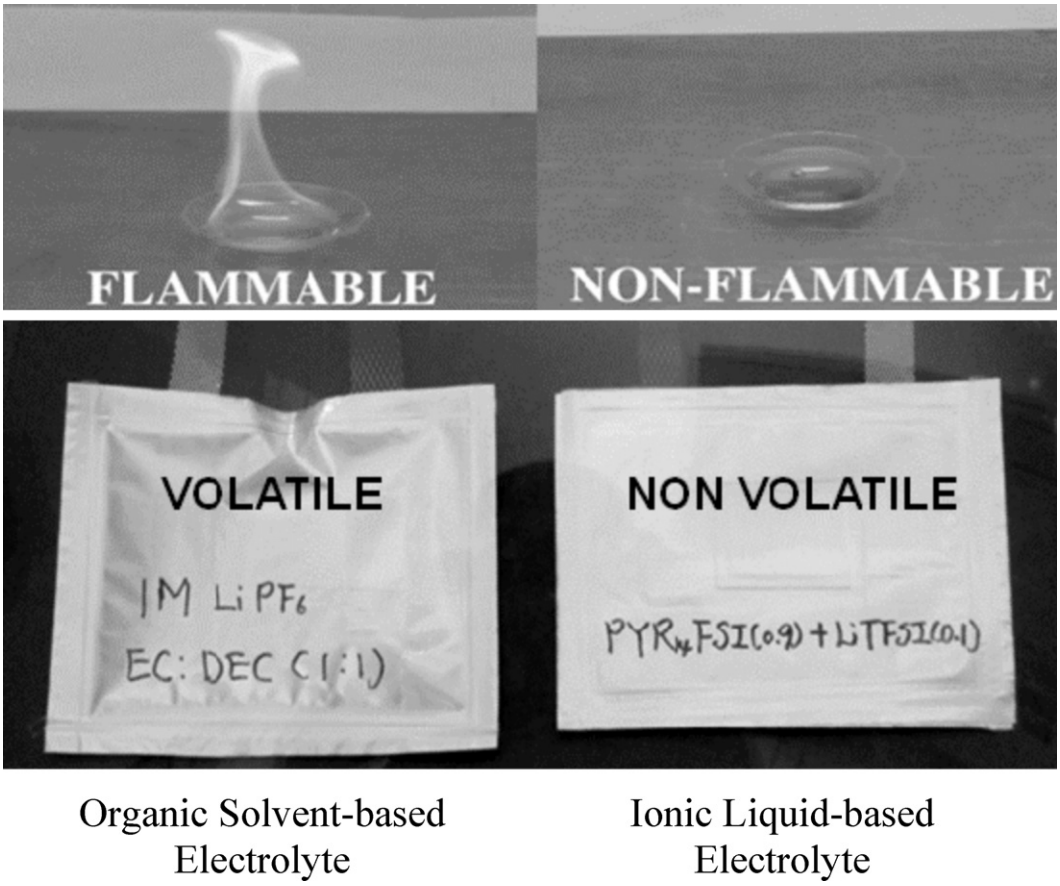


**Fig. 1.** Flammability and volatility tests performed on organic solvent- and ionic liquid-based electrolytes. The upper images show the results of the flammability tests performed by exposing the two electrolytes to a LPG flame for 2 s. The lower images show the effect of vacuum on two identical pouch cells based on the different electrolytes placed under vacuum in the same vacuum chamber.

electrode manufacturing. In fact, present electrode manufacturing frequently involves the use of polyvinyliden-di-fluoride (PVdF) binder that requires the use of volatile organic compounds for the processing such as N-methyl-pyrrolidone (also named as NMP). These solvents are not only expensive, but also environmentally harmful and toxic thus introducing safety concerns in the manufacturing process. In addition, PVdF is a relatively costly polymer (industrial cost in the multiton scale is around 15–18 EUR $kg^{-1}$) and not easily disposable at the end of the battery life. For these reasons, the substitution of PVdF with a cheaper and more environmental-friendly binder would be very welcome.

In the last few years, alternative binders have been introduced for the manufacturing of anodes for lithium ion-batteries [15–27]. Between them, one of the most interesting is certainly the sodium salt of CarboxyMethylCellulose (CMC). CMC is produced by the insertion of carboxymethyl groups in natural cellulose. The presence of these groups makes the CMC water-soluble. This is certainly the greatest advantage of CMC since it allows the processing in aqueous slurries rather than in polluting, health and environment unfriendly, volatile organic compound-based slurries. The second great advantage of CMC resides in the easy disposability at the end of the battery life. Once the electrode is extracted, the active electrode material can be easily recovered by pyrolysis of the binder. Last but not least, the material cost. CMC industrial price is about 1–2 EUR $kg^{-1}$, i.e., about one order of magnitude lower than PVdF.

Recent works showed that CMC can be used as a replacement for PVdF in lithium iron phosphate ($LiFePO_4$) based electrodes [28–32]. The excellent results of these studies indicated that the introduction of CMC as binder is a viable and extremely promising solution toward the environment-friendly preparation of cathode electrodes based on $LiFePO_4$ as the active material. If the use of non-volatile ionic liquid-based electrolytes is also contemplated in the battery system, than the possibility to develop safer and greener lithium ion batteries is fully open, where not only the safety of the systems, but also the safety of the overall batteries preparation process is enhanced.

This manuscript is focused on the study of the performance of a lithium ion battery containing CMC as binder both for cathode and anode, using an electrolytic solution based on ionic liquids. The considered battery contains $Li_4Ti_5O_{12}$ and $LiFePO_4$ at the anode and cathode, respectively, which are also considered to be safe and environment-friendly materials. The electrolytic solution is based on the ionic liquid $PYR_{14}FSI$. The results of the electrochemical tests carried out at 20 °C and 40 °C on this safe and green battery are reported in this paper.

## 2. Experimental

### 2.1. Synthesis of $PYR_{14}FSI$

The $PYR_{14}FSI$ room temperature ionic liquid was synthesized and dried as reported in [11].

### 2.2. TGA

Thermo gravimetric measurements were carried out using a Q 5000 IR TGA instrument (TA Instruments). High-temperature platinum pans loaded with 10–20 mg samples were used for the tests.

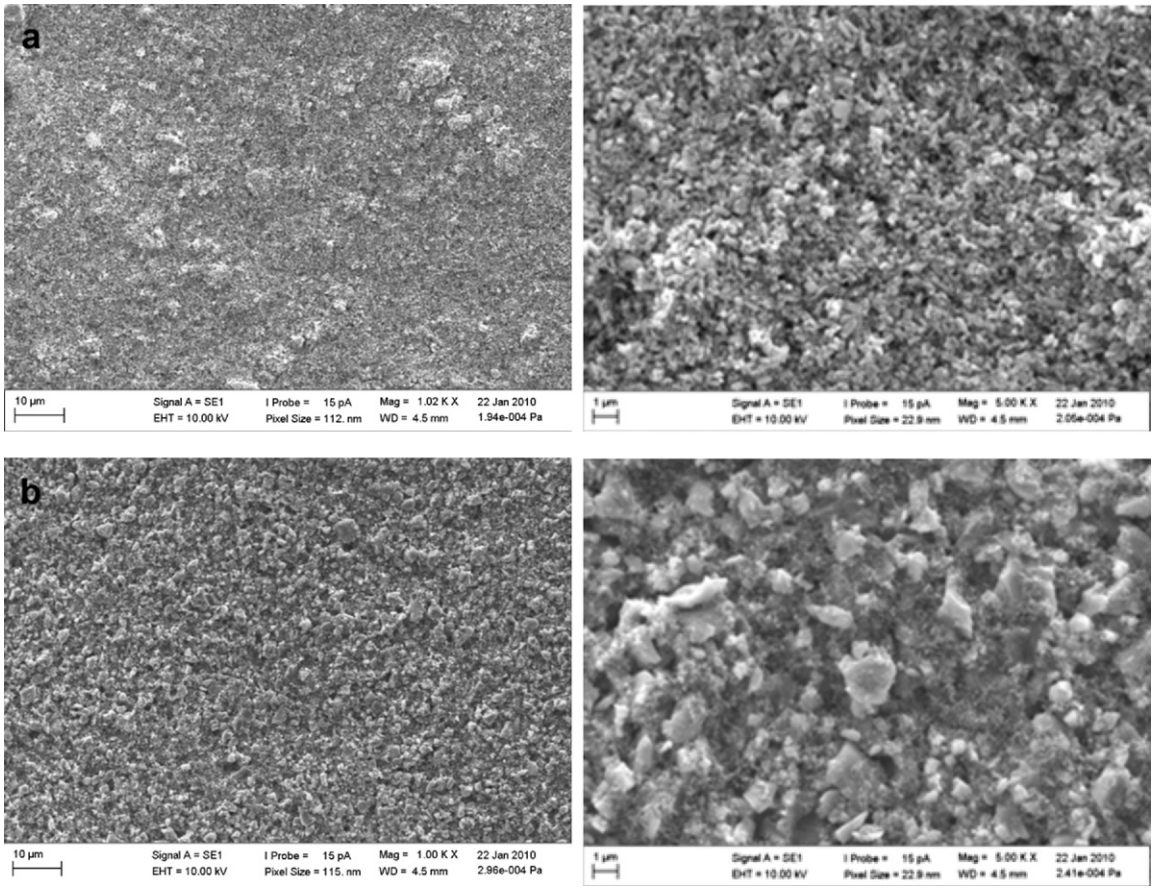


**Fig. 2.** SEM images of $LiFePO_4$ electrodes based on CMC (upper panels) and $Li_4Ti_5O_{12}$ electrodes based on CMC (lower panels).

All samples, previously dried to remove the adsorbed water, were heated from room temperature to 800 °C with a heating rate of 5 °C $min^{-1}$, using nitrogen as purge gas (10 ml $min^{-1}$).

### 2.3. Electrode preparation

Commercial carbon-coated $LiFePO_4$ (average particle size: 0.3 μm; carbon content: 2.3 wt.%) and uncoated $Li_4Ti_5O_{12}$ (average particle size: 2 μm) (both from Südchemie, Germany) were used as delivered. Sodium-CarboxyMethylCellulose (CMC, Dow Wolff Cellulosics, Walocel CRT 2000 PPA 12) with a degree of substitution of 1.2 was used as the binder while the conducting agent carbon black was Super-P (TIMCAL, average particle size: 30 nm).

Lithium titanate and lithium iron phosphate electrodes were prepared following a common recipe. CMC was firstly dissolved in deionized water at room temperature by magnetic stirring. The required amount of Super-P was then added to the aqueous solution containing CMC and the mixture was ball milled in a zirconia jar loaded with 5 mm zirconia balls (the weight of the balls corresponded to three times the total weight of the dry electrode components). The mixing was performed for more than 1 h with a planetary ball mill (Fritsch, Pulverisette 4; rotation speed: 800 rpm). The selected amount of active material was then added into the mixture and the slurry was homogenized by ball milling at RT for 1 additional hour. During the preparation of the $Li_4Ti_5O_{12}$, 0.025 g of formic acid per gram of active material was introduced to neutralize (pH = 7) the slurry, which had a very basic character [33].

The so-obtained slurries were cast on aluminum foils (20 μm, purity >99.9%) by using a laboratory scale blade coater. The wet coated electrodes were immediately pre-dried in an atmospheric oven with stagnant air at 80–100 °C for 1 h. From the so-obtained electrode tapes, electrodes with an area of 4 $cm^2$ were prepared. The prepared electrodes were dried at 180 °C under vacuum for 24 h. The composition of the dried cathode electrodes was 88 wt.% $LiFePO_4$, 8 wt.% Super-P and 4 wt.% of CMC while that of the anode electrodes was 87 wt.% $Li_4Ti_5O_{12}$, 8 wt.% Super-P and 5 wt.% of CMC. The average mass loading of the electrodes was about 4.0 mg $cm^{-2}$.

### 2.4. Electrochemical tests

All the electrochemical tests were carried out in lab-made pouch cells assembled in a dry-room (R.H. < 0.1% at 20 °C). An electrolytic solution containing 0.1LiTFSI–0.9 $PYR_{14}FSI$ (where 0.1 and 0.9 represent the molar ratio of the components) with water content of less than 5 ppm was used in all tests.

Full-cells were realized by sandwiching an impregnated separator layer (Freudenberg, FS2190) between the anodic and cathodic electrodes (cell area 4 $cm^2$).

Half-cells were realized by facing a cathodic (or anodic) electrode with a lithium foil (Chemetall, 0.05 mm thick) counter electrode. A glassy fiber separator (Whatman) impregnated with the electrolyte was used in these cells because of the anomalous lithium dendritic growth observed on the FS2190 separators in contact with the lithium metal electrode.

The constant current (CC) tests were carried at 20 ± 2 °C with a MACCOR Battery tester 4300. Variable temperature tests were also performed at 40 °C and 60 °C using a climatic chamber Binder NK53.

## 3. Results and discussion

Fig. 2 shows the SEM images of the $LiFePO_4$ (a) and $Li_4Ti_5O_{12}$ (b) electrodes at two different magnifications. The low magnifi-

cation picture of the $LiFePO_4$ electrode reveals the formation of small bumps due to the presence of secondary particles (or particle aggregates) smaller than 10 μm. However, the $LiFePO_4$ primary particles are smaller than 1 μm. In the case of $Li_4Ti_5O_{12}$ the particles appear larger (more than 2 μm), but almost no secondary particles (aggregates) are visible. It is important to note that both electrodes display high compactness, even if they were not subjected to any post-coating process (e.g. roll pressing). This benefit, which originates from the substantial shrinkage of cellulose during the final drying step at elevated temperatures [32], might result in a simplification of the manufacturing process with a consequent reduction of process time and cost. Clearly this property would represents an additional advantage of the use of CMC as binder, however, tests on pre-pilot coating lines are needed to verify this option.

Fig. 3a presents the TGA curves of the inert electrode components, i.e., the electronic conductive additive, Super P, and the binder, CMC. The tests were performed under nitrogen flow using a temperature increase rate of 5 °C $min^{-1}$. While the Super P did not show any detectable weight loss over the entire temperature range investigated, the CMC showed a marked decomposition step above 200 °C, which depended on the preliminary processing. The thermal investigation indicates that air-exposed CMC powder takes up about 7 wt.% of water, which is released in the temperature range between 50 °C and 250 °C. The thermal decomposition of CMC is seen to begin above 400 °C with a weight loss of about 43 wt.% observed at 500 °C. Above 500 °C only a slight weight loss is observed and at 600 °C, the remaining weight for the air-exposed CMC is 43.5 wt.%. On the other hand, the CMC sample pre-dried at 180 °C showed almost no weight loss below 200 °C. The small weight loss detected around 100 °C with the CMC dried at 180 °C is to be associated with a slight contamination during sample loading in the TG equipment. Also interesting to notice is the apparently enhanced stability of the pre-dried CMC, which is obviously due to the partial decomposition taking place during the drying step at 180 °C. As a matter of fact, the pre-dried CMC showed, before the TGA experiment, a slight brownish coloration. However, apart from the onset of the thermal decomposition, no other differences were detected in the pre-dried material with respect to air-exposed one. The residual weight for the air-dried material was 46.3 wt.%, which matched very well with the 43.5 wt.% detected in the air-exposed one considering the initial water content of this latter material.

In Fig. 3b are presented the TGA curves detected for the $Li_4Ti_5O_{12}$ composite electrode (the sample was scratched from a coated electrode) as well as the pristine $Li_4Ti_5O_{12}$ powder (as received from the supplier and dried at 180 °C). This latter material exhibited an overall weight loss of only 0.5 wt.% at 600 °C, mostly taking place between 200 °C and 300 °C as a result of the release of strongly adsorbed or even chemically bound surface water molecules. The weight loss behavior of the $Li_4Ti_5O_{12}$ composite electrode seems to indicate that these water molecules are eliminated by the electrode drying step at 180 °C. As a matter of the fact, the overall weight loss of the composite electrode sample slightly exceeded 1.5 wt.%, which is in very good agreement with the weight loss of the 5 wt.% CMC present in the electrode (see pre-dried curve in Fig. 3a). The appearance of the thermal decomposition onset at lower temperature is certainly due to a catalytic effect on the CMC decomposition exerted by the oxide particles.

Fig. 3c presents the thermal stability curves of pristine, carbon coated $LiFePO_4$ powder (as received from the supplier and dried at 180 °C) and the $LiFePO_4$ composite electrode. Pristine $LiFePO_4$ showed an early onset of the weight loss with a first discrete step located between 120 °C and 150 °C. However, the overall total weight loss was limited to less than 1 wt.% at 600 °C. The thermal stability curve of the composite electrode resembles the combination of those of the pristine materials ($LiFePO_4$ and CMC), however, a total weight loss of only 2 wt.% is detectable at 600 °C. This value is

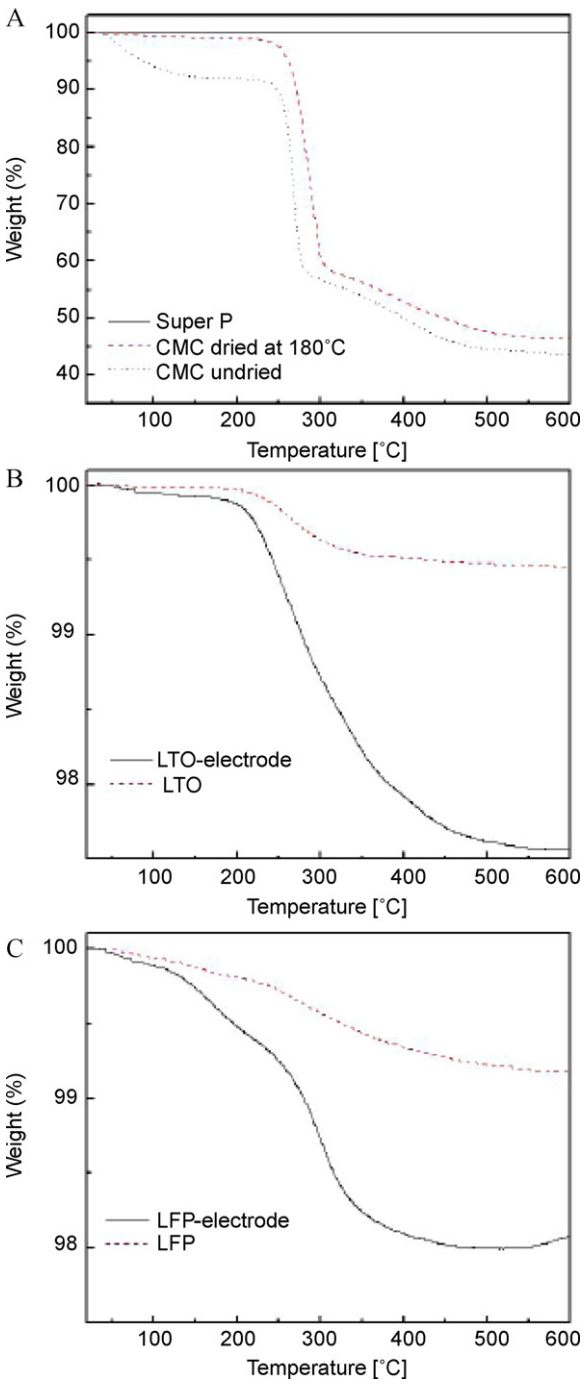


**Fig. 3.** TG weight loss profiles of (a) CMC powder and Super P, (b) $Li_4Ti_5O_{12}$ powder and composite electrode and (c) $LiFePO_4$ powder and composite electrode.

about 1 wt.% lower than that expected from the weight losses of the pristine materials but matches very well with the weight loss due to CMC only. The reason of this behavior is not clear yet, however, it is reasonable to suggest that the slight weight loss in the low temperature region area is due to some catalytic effect exerted by the active material powders on the decomposition of CMC. Nevertheless, considering that the CMC content in the $LiFePO_4$ and $Li_4Ti_5O_{12}$ composite electrodes is 4 wt.% and 5 wt.%, respectively, and that the weight loss of pre-dried CMC at 600 °C is 46.5%, it is easy to see how the experimentally detected losses (respectively 2 wt.% and 2.4 wt.%) match the theoretical values.

To summarize the thermal analysis results, it is clear that CMC is the less thermally stable electrode component. The pristine mate-

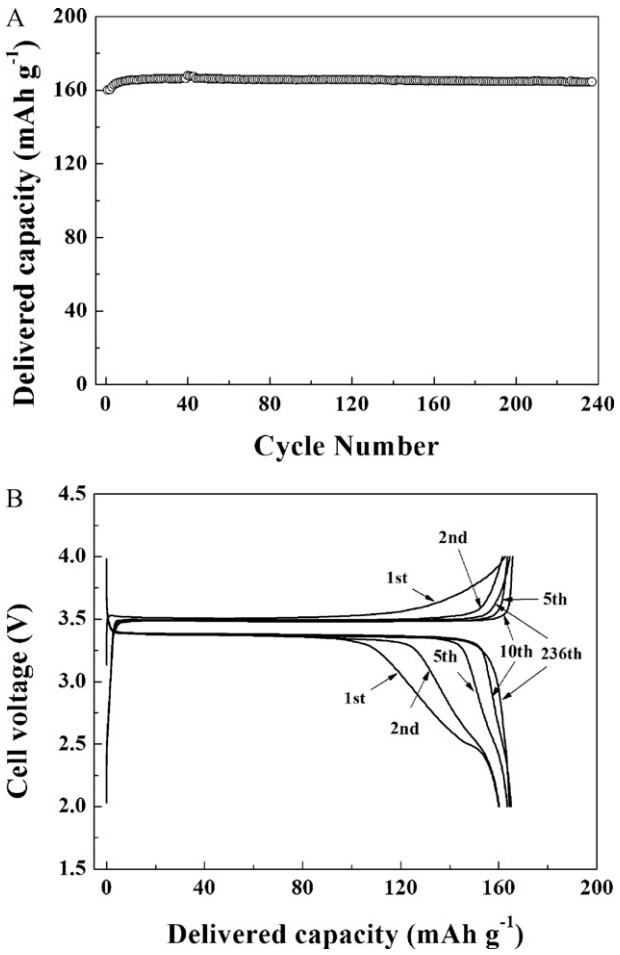


**Fig. 4.** $LiFePO_4$ electrodes in half-cell (Li anode) configuration with ($0.9PYR_{14}FSI$–0.1LiTFSI) electrolyte: delivered capacity vs. cycle number (a) and voltage profile vs. specific capacity of a few selected cycles (b) recorded at 20 °C and 0.1 C rate.

rials and, especially, Super P have excellent thermal stabilities. However, since major decomposition processes in both composite electrodes only take place above 200 °C, it can be assumed that the drying temperature of 180 °C does not affect the materials during the electrode manufacturing process. Moreover, the results of the thermal analysis indicated that the prepared electrodes, if used in combination with high thermally stable electrolytes (e.g. ionic liquids), could be used without problem also at high temperatures.

The electrochemical performance of the anodic ($Li_4Ti_5O_{12}$-based) and cathodic ($LiFePO_4$-based) composite electrodes was tested at 20 °C (unless differently specified) in half-cell and full lithium ion configurations using an ionic liquid-based electrolyte ($0.9PYR_{14}FSI$–0.1LiTFSI). As indicated above, $PYR_{14}FSI$ represents nowadays one of the most attractive ionic liquids for use as electrolyte in lithium-ion batteries since it displays high conductivity (>4 mS $cm^{-1}$ at 20 °C), and an overall electrochemical stability window of more than 5.5 V [13].

Fig. 4a shows the results of the constant current (CC) tests of a $LiFePO_4$ composite electrode in half-cell configuration, carried out at a current density corresponding to 0.1 C rate and 20 °C. As shown in the figure, the electrode displayed an initial specific capacity of about 160 mAh $g^{-1}$. During the initial 10 cycles the specific capacity delivered by the electrode slightly increased to reach 165 mAh $g^{-1}$ and than it remained constant for more than 200 cycles. As shown in Fig. 4b, the voltage profile of the electrode also changes upon cycling, especially in the initial 10 cycles where the typical plateau of $LiFePO_4$ cathodes around 3.4 V vs. $Li/Li^+$ is seen to substantially extend in spite of a second plateau at 2.5 V vs. $Li/Li^+$ clearly appearing in the first cycle. In the following cycles the voltage profile of the $LiFePO_4$ electrode does not show any major change as previously indicated by the practically constant delivered capacity (ca. 165 mAh $g^{-1}$).

The change of delivered capacity upon cycling is easily explained by the slow wetting of the electrode porosity wetting associated with the higher viscosity of IL-based electrolytes with respect to conventional, organic solvent-based electrolytes. This kind of behavior was, in fact, already observed for $LiFePO_4$ based electrode in IL-based electrolyte [34]. However, it is important to note that the number of cycles necessary to reach the highest value of specific capacity was much higher (in the order of 100 cycles) in other ILs-based electrolyte than in ($0.9PYR_{14}FSI$–0.1LiTFSI). Moreover, the specific capacity observed for the same kind of electrode in other IL-based electrolytes were always much lower (50 mAh $g^{-1}$ or more) than those observed in ($0.9PYR_{14}FSI$–0.1LiTFSI). For that, the electrolyte ($0.9PYR_{14}FSI$–0.1LiTFSI) appears to be very promising for the use in combination with $LiFePO_4$, with performance comparable with that obtained in conventional, organic solvent-based electrolytes. The appearance of the second plateau at 2.5 V vs. $Li/Li^+$ seems also to be associated with slower kinetics as indicated by the lithium extraction overvoltage arising toward the end of the initial, few lithium deinsertion cycles. Most likely, the hydrophilic cellulose is at least initially limiting the active material particles wetting by the ionic liquid electrolyte. Nevertheless, upon cycling this anomaly fully disappears as indicated by the long-term cycling behavior of the CMC-based, $LiFePO_4$ composite electrode reported in Fig. 4.

Similar galvanostatic cycling tests were also performed on $Li_4Ti_5O_{12}$ composite electrodes. Fig. 5a shows the delivered capacity vs. cycle number detected during the CC test (0.1 C rate at 20 °C). As shown in the figure, during the first lithium intercalation the electrode displayed a specific capacity of about 160 mAh $g^{-1}$. During the following deintercalation–intercalation cycle, however, the capacity slightly decrease to a value of ca. 150 mAh $g^{-1}$ to remain than constant for 100 cycles. The difference from the first and the following cycles is clearly visible in Fig. 5b, where the voltage profiles of the electrode are shown. Clearly, some irreversibility is observed between the first lithium insertion and deinsertion steps. This irreversibility, which was not observed in PVDF-based $Li_4Ti_5O_{12}$ composite electrodes (results not shown), is certainly associated with the aqueous (CMC-based) electrode processing which might cause some reversible surface modification. Nevertheless, it is important to notice that the lithium insertion–deinsertion process becomes very reversible after the first cycle. In addition, the specific delivered capacity and the cycling stability obtained with the CMC-based $Li_4Ti_5O_{12}$ composite electrodes in ($0.9PYR_{14}FSI$–0.1LiTFSI) electrolyte are comparable with those obtained from composite electrodes, using PVDF as the binder, in conventional, organic solvent-based electrolytes.

It is well known that one among the safest, if not the safest, lithium-ion battery chemistries is obtained using $Li_4Ti_5O_{12}$ and $LiFePO_4$ electrode materials [35–37]. However, the use of non-flammable, non-volatile, ionic liquid electrolytes (such as $0.9PYR_{14}FSI$–0.1LiTFSI) is expected to further improve the already high safety of such systems. Moreover, considering the performance of the single electrodes in ($0.9PYR_{14}FSI$–0.1LiTFSI), it is also reasonable to suppose that this safe system would also be able to display very high performance. For these reasons, we prepared a lithium-ion batteries containing $Li_4Ti_5O_{12}$ and $LiFePO_4$ as active materials, CMC as binder and ($0.9PYR_{14}FSI$–0.1LiTFSI) and we investigated the performance of this systems at RT.

Taking into account the performance of each electrode and their behavior during the first cycles, cells with an anode/cathode capacity ratio of about 1 (0.68 mAh $cm^{-2}$ $Li_4Ti_5O_{12}$ vs. 0.67 mAh $cm^{-2}$

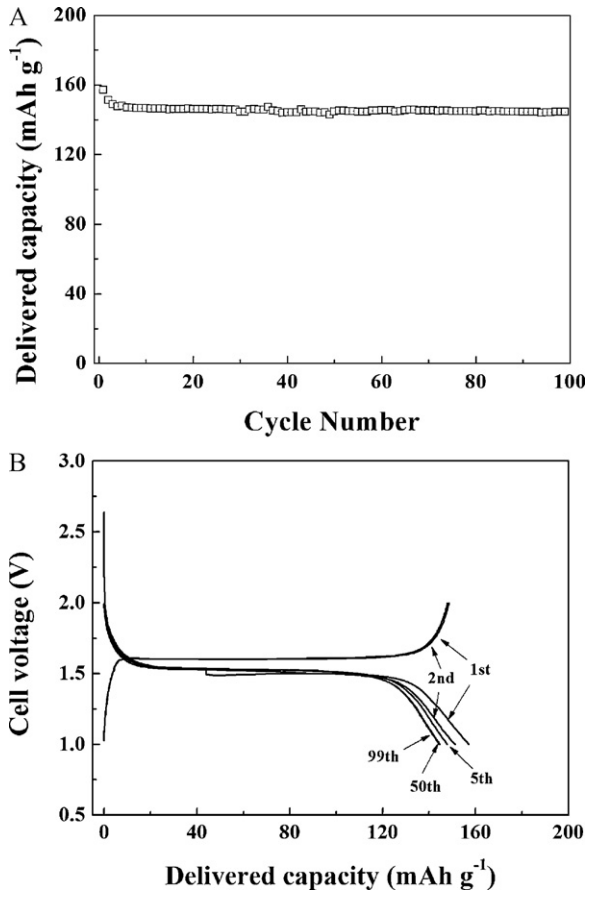


**Fig. 5.** $Li_4Ti_5O_{12}$ electrodes in half-cell (Li anode) configuration with ($0.9PYR_{14}FSI$–0.1LiTFSI) electrolyte: delivered capacity vs. cycle number (a) and voltage vs. specific capacity of a few selected cycles (b) recorded at 20 °C and 0.1 C rate.

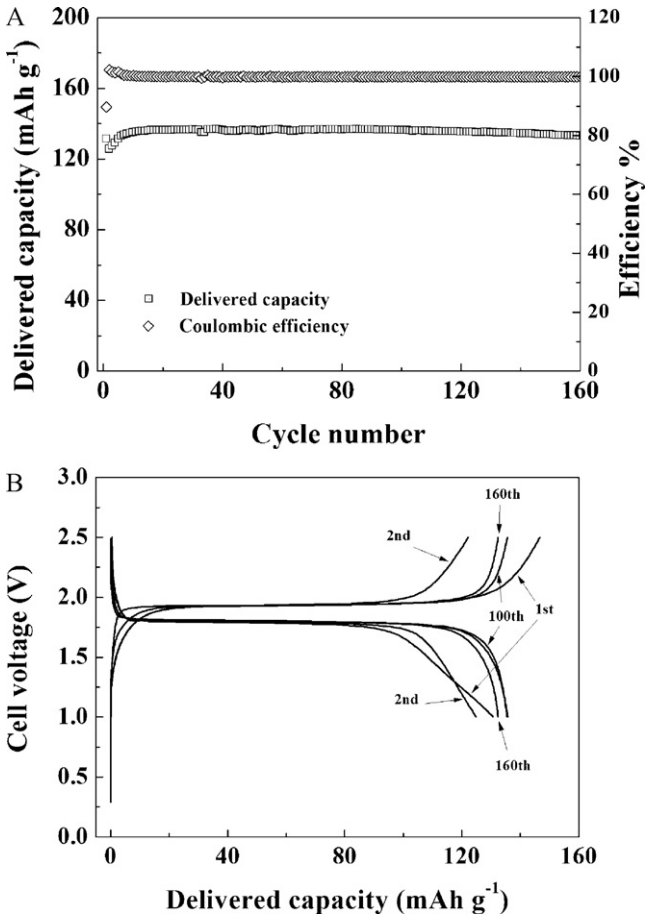


**Fig. 6.** Lithium-ion $Li_4Ti_5O_{12}$/$LiFePO_4$ cell with ($0.9PYR_{14}FSI$–0.1LiTFSI) electrolyte: delivered capacity vs. cycle number (a) and voltage vs. specific capacity of a few selected cycles (b) recorded at 20 °C and 0.1 C rate.

$LiFePO_4$) were assembled and tested. Fig. 6a shows the results of the charge–discharge tests carried out on one of these cells at a current density corresponding to 0.1 C rate and room temperature (20 °C). After 160 full charge–discharge cycles, the assembled lithium-ion battery delivered a discharge capacity higher than 135 mAh $g^{-1}$ (cathode and anode have approx. the same active material loading) with the charge efficiency being higher than 99%. In the first cycle the battery showed a discharge capacity of 135 mAh $g^{-1}$. The charge efficiency was about 90%, i.e., in good agreement with the first cycle efficiency of the $Li_4Ti_5O_{12}$ electrodes. At the second cycle the specific capacity slightly decrease to a value of ca. 125 mAh $g^{-1}$, but the efficiency increased to 100%. In the following cycles the delivered capacity increased till a value close to 140 mAh $g^{-1}$ and the efficiency remain constant at 100%. After 160 cycles the system displays a discharge specific capacity of about 135 mAh $g^{-1}$. The changes taking place upon cycling the lithium-ion cell are well visible when the voltage profiles of the cell are considered. As shown in Fig. 6b, from the first to the second cycles the voltage profiles (charge and discharge) significantly change and become shorter, and the capacity associated with the processes decrease. To the contrary, from the second to the hundredth cycle the plateaus associated with the charge–discharge process become longer and the specific capacity increase. This behavior is certainly related with the behavior of the single electrodes during the first cycle. As described above in the text, during the first 4–5 cycles the $Li_4Ti_5O_{12}$ electrode normally shows a slight decrease of capacity, while in these initial cycles $LiFePO_4$ electrode shows an increase of capacity due to the improved electrode wetting and the change in the electrode surface. As a result, the cell shows a decrease of capacity from the first to the second cycle and an improvement of specific capacity and efficiency in the following cycles.

The performance of the investigated battery is certainly very promising both in term of specific capacity and cycling stability. As a matter of fact, the delivered capacity, the efficiency and the cycling stability of the investigated battery are comparable with those of $Li_4Ti_5O_{12}$/$LiFePO_4$ systems working in conventional electrolyte. At the best of our knowledge, this battery represents the first example of a systems using CMC as binder for both electrode and an electrolytic solution based on ionic liquids able to display such performance.

Considering these promising results, we also evaluated the battery performance at higher rate and temperatures. We carried out a test consisting of a sequence of cycles performed at 20 °C and 0.1 C (10 cycles), at 40 °C and 0.2 C (10 cycles), and at 60 °C and 0.5 C (10 cycles). After this sequence, a second sequence of cycles at 20 °C and 0.1 C (10 cycles) and at 40 °C and 0.2 C (10 cycles) was performed. The aim of the second sequence was to verify if the cycling at high temperature (60 °C) could negatively affect the battery performance. The results reported in Fig. 7a show that when the temperature was increased to 40 °C the batteries was able to display better performance (more than 150 mAh $g^{-1}$) than at 20 °C (about 140 mAh $g^{-1}$) even if the rate of charge–discharge rate was two times higher. At 60 °C the battery displayed a specific capacity of 130 mAh $g^{-1}$ at 0.5 C. Although a slight fading is observed during cycling at 60 °C, the cell performance is very interesting because of the relative high rate used and, even more important, because cycling at 60 °C cannot be safely achieved with conven-

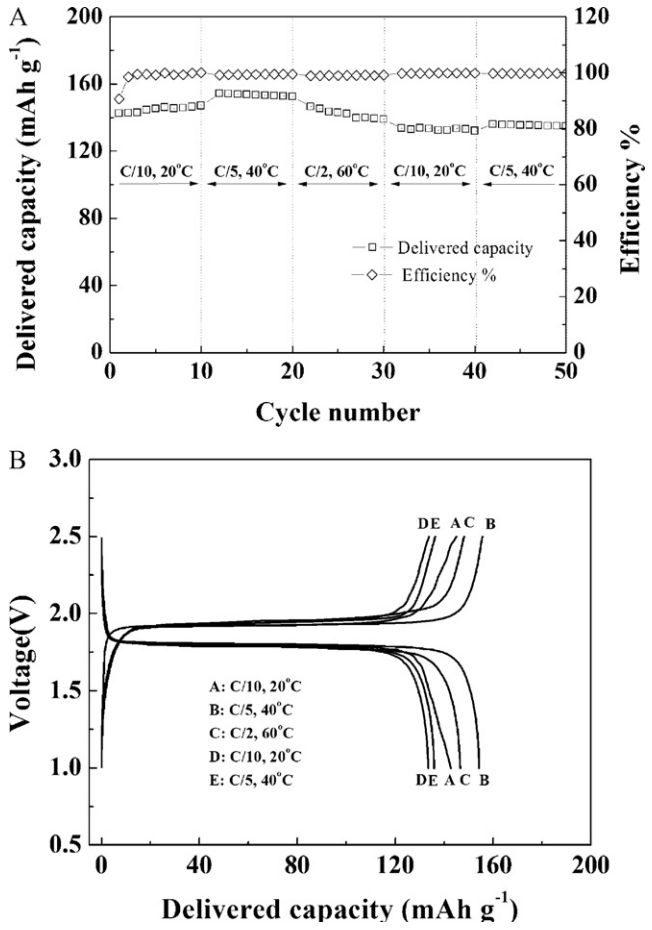


**Fig. 7.** Lithium-ion battery $Li_4Ti_5O_{12}$/$LiFePO_4$ cell with (0.9$PYR_{14}$FSI–0.1LiTFSI) electrolyte: delivered capacity vs. cycle number (a) and voltage vs. specific capacity of a few selected cycles (b) recorded at 20 °C and 0.1 C, 40 °C and 0.2 C rate, and 60 °C and 0.5 C rate.

tional, organic solvent-based electrolytes. Moreover, it is important to note that when the temperature was decreased again to 20 °C the battery was able to maintain good performance with only small capacity and power losses. As a matter of fact, during the second sequence of cycles the battery displayed a specific capacity higher than 130 mAh $g^{-1}$, indicating that the cycle test at higher temperature did not substantially damage the cell. This can also be observed in Fig. 7b, where the voltage profiles detected at different temperatures during the first and the second sequence are compared.

The results of these tests show that the lithium-ion battery made with CMC-based $Li_4Ti_5O_{12}$ and $LiFePO_4$ composite electrodes and (0.9$PYR_{14}$FSI–0.1LiTFSI) displayed good performance at 40 °C and 60 °C and higher C-rates. Even more important, the cycling at elevated temperature (60 °C) appears to only slightly affect the Li-ion cell performance.

Work is now in progress to further investigate the characteristics and the performance of this safe and high performance lithium-ion battery. Particular attention will be dedicated to the evaluation of the battery performance at higher C-rate and operating temperature.

## 4. Conclusion

The use of CMC as the binder material for composite electrode together with electrolytic solutions based on ionic liquids appears as a viable and extremely promising solution for the development of greener and safer batteries.

CMC allows the use of aqueous slurries and yields to low porosity electrodes. These are, of course, important advantages in view of the realization of greener and cheaper batteries since no volatile organic compounds are involved in the processing and a reduced need of the post-coating treatment (roll pressing), presently needed in PVDF-based electrode manufacturing. The introduction of CMC in the battery technology would bring benefits in term of reducing the production costs and time. These advantages would be further extended by CMC lower cost and easier disposability at the end of the battery life with respect to PVDF.

$Li_4Ti_5O_{12}$ and $LiFePO_4$ electrodes employing CMC as the binder are thermally stable up to 200 °C and display performance comparable to that of PVDF-based electrodes. Their use in combination with ionic liquid-based electrolytic solution (0.9$PYR_{14}$FSI–0.1LiTFSI) is also showing very promising performance. $LiFePO_4$ electrodes display a specific capacity of about 160 mAh $g^{-1}$ stable for more than 240 cycles, while $Li_4Ti_5O_{12}$ electrodes display a specific capacity of about 150 mAh $g^{-1}$ stable for more than 100 cycles.

Lithium-ion $Li_4Ti_5O_{12}$/$LiFePO_4$ cells employing CMC as electrode binder and ionic liquid-based electrolyte (0.9$PYR_{14}$FSI–0.1LiTFSI) were realized and found to deliver (at room temperature) a discharge capacity of about 140 mAh $g^{-1}$ (with a charge efficiency higher than 99%) for 160 cycles. The room temperature performance of these cells is somehow limited to low C rates and it is certainly lower than that obtained for similar electrodes in conventional (organic solvent-based) electrolytes, due to the higher viscosity of the IL-based electrolyte. However, these lithium-ion cells display high performance also at 40 °C (more than 150 mAh $g^{-1}$ at 0.2 C) and 60 °C (130 mAh $g^{-1}$ at 0.5 C) without any major degradation.

To the best of our knowledge, this battery chemistry is innovative and represents the first example of an easy to recycle system. In fact, halides are only present in the easily recyclable (non-volatile, non-flammable) ionic liquid-based electrolyte. Electrode materials can be easily separated into their components by dissolution in water of the binder thus allowing for a full recovery of the metallic current collectors. As a final step of the recycling procedure, the binder and the carbon additive could be fired to leave the active materials available for regeneration and reuse.

## Acknowledgments

The authors wish to thank the financial support of the European Commission within the FP6 STREP Projects ILLIBATT (Contract no. NMP3-CT-2006-033181).

## References

[1] W.A. van Schalkwijk, B. Scrosati, Advanced in Lithium-Ion Batteries, Kluwer Academic/Plenum Publisher, 2002.
[2] G.-A. Nazri, G. Pistoia, Lithium Batteries, Kluwer Academic/Plenum Publisher, 2004.
[3] B. Garcia, S. Lavallée, G. Perron, C. Michot, M. Armand, Electrochim. Acta 49 (2004) 4583.
[4] S.-Y. Lee, S.K. Kim, S. Ahn, Electrochem. Commun. 10 (1) (2008) 113.
[5] A. Guerfi, S. Duchesne, Y. Kobayashi, A. Vijh, K. Zaghib, J. Power Sources 175 (2) (2008) 866.
[6] J.-H. Shin, W.A. Henderson, S. Scaccia, P.P. Prosini, S. Passerini, J. Power Sources 156 (2) (2006) 560.
[7] M. Ishikawa, T. Sugimoto, M. Kikuta, E. Ishiko, M. Kono, J. Power Sources 162 (1) (2006) 658.
[8] A. Lewandowski, A. Świderska-Mocek, J. Power Sources 171 (2) (2007) 938.
[9] M. Holzapfel, C. Jost, P. Novák, Chem. Commun. (2004) 2098.
[10] S.F. Lux, M. Schmuck, G.B. Appetecchi, S. Passerini, M. Winter, A. Balducci, J. Power Sources 192 (2010) 606.
[11] G.B. Appetecchi, M. Montanino, A. Balducci, S.F. Lux, M. Winter, S. Passerini, J. Power Sources 192 (2009) 599.
[12] S.F. Lux, M. Schmuck, S.S. Jeong, S. Passerini, M. Winter, A. Balducci, Int. J. Energy Res. 34 (2010) 97.

[13] P. Johansson, L.E. Fast, A. Matic, G.B. Appetecchi, S. Passerini, J. Power Sources 195 (2010) 2074.
[14] A. Balducci, M. Schmuck, W. Kern, B. Rupp, S. Passerini, M. Winter, ECS Trans. 11 (29) (2008) 109.
[15] N.S. Hochgatterer, M. Schweiger, S. Koller, P. Raimann, T. Wohrle, C. Wurm, M. Winter, Electrochem. Solid State Lett. 11 (5) (2008) A76.
[16] M. Holzapfel, H. Buqa, W. Scheifele, P. Novak, F.M. Petrat, Chem. Commun. (2005) 1566.
[17] J. Li, R.B. Lewis, J.R. Dahn, Electrochem. Solid-State Lett. 10 (2007) A17.
[18] M. Yoshio, T. Tsumura, N. Dimov, J. Power Sources 163 (2006) 215.
[19] N. Dimov, Y. Xia, M. Yoshio, J. Power Sources 171 (2007) 886.
[20] J.H. Lee, S. Lee, U. Paik, Y.M. Choi, J. Power Sources 147 (2005) 249.
[21] J.H. Lee, U. Paik, V.A. Hac kley, Y.M. Choi, J. Electrochem. Soc. 152 (2005) A1763.
[22] J.H. Lee, U. Paik, V.A. Hac kley, Y.M. Choi, J. Power Sources 161 (2006) 612.
[23] S.S. Zhang, K. Xu, T.R. Low, J. Power Sources 138 (2004) 226.
[24] M. Gaberscek, M. Bele, J. Drofenik, R. Dominko, S. Pejovnik, J. Power Sources 97–98 (2001) 67.
[25] J. Drofenik, M. Gaberscek, R. Dominko, F.W. Poulsen, M. Mogensen, S. Pejovnik, J. Jamnik, Electrochim. Acta 48 (2003) 883.
[26] Y.M. Choi, K.H. Kim, U. Paik, WO Pat 04/0258991 A1 (2004).
[27] Y.M. Park, T.B. Oh, D.H. Lee, K.W. Cho, WO Pat 05/0158624 A1 (2005).
[28] W. Porcher, B. Lestriez, S. Jouanneau, D. Guyomard, J. Electrochem. Soc. 156 (3) (2009) A133.
[29] W. Porcher, P. Moreau, B. Lestriez, S. Jouanneau, D. Guyomard, Electrochem. Solid-State Lett. 11 (1) (2008) A4.
[30] W. Porcher, P. Moreau, B. Lestriez, S. Jouanneau, F. Le Cras, D. Guyomard, Ionics 14 (2008) 583.
[31] J.H. Lee, J.S. Kim, Y.C. Kim, D.S. Zang, U. Paik, Ultramicroscopy 108 (2008) 1256.
[32] S.F. Lux, F. Schappacher, A. Balducci, S. Passerini, M. Winter, J. Electrochem. Soc. 157 (3) (2010) A320.
[33] D.R. Simon, E.M. Kelder, M. Wagemaker, F.M. Mulder, J. Schoonman, Solid State Ionics 177 (2006) 2759.
[34] S.F. Lux, S.S. Jeong, G.-T. Kim, S. Passerini, M. Winter, A. Balducci, ECS Trans. 25 (36) (2010) 21.
[35] B. Scrosati, J. Garche, J. Power Sources 2419–2430 (195) (2010) 9.
[36] T. Ohzuku, K. Ariyoshi, S. Yamamoto, Y. Makimura, Chem. Lett. 1270 (2001) 12.
[37] P. Reale, S. Panero, B. Scrosati, J. Garche, M. Wohlfart-Meherens, M. Wachtler, J. Electrochem. Soc. 151 (2004) 12.